Indonesian Journal of Biotechnology

VOLUME 30(1), 2025, 1-11 | RESEARCH ARTICLE

# Characterization and antibacterial activity of biosynthesized silver nanoparticles using *Stachytarpheta jamaicensis* leaf extract as bioreduction

**Sandy Samsul Bahry[1], Ari Susilowati[1,*], Artini Pangastuti[1]**

Department of Biology, Faculty of Mathematics and Natural Sciences, Universitas Sebelas Maret, Jl. Ir. Sutami No. 36A, Kentingan, Surakarta, Central Java 57126, Indonesia
*Corresponding author: arisusilowati@staff.uns.ac.id

**SUBMITTED** 28 August 2023 **REVISED** 28 October 2024 **ACCEPTED** 20 November 2024

**ABSTRACT** Their nanometer size, broad spectrum, and antibacterial mechanism give silver nanoparticles (NPAg) the potential to be used to inhibit the growth and spread of methicillin-resistant *Staphylococcus aureus* (MSRA) in medical devices. Synthesis of AgNPs from *Stachytarpheta jamaicensis* leaf extract is considered more environmentally friendly and has low production costs. The objective of this study was to investigate the properties and antibacterial potential of AgNPs by utilizing *S. jamaicensis* leaf extract at concentrations of 0.5%, 1.0%, and 1.5% in a 1 mM $AgNO_3$ precursor. Nanoparticle characterization was performed on the AgNP supernatant obtained by centrifuging the synthesis solution at 100 rpm for 5 min. Characterization of the NPAg size was confirmed by surface plasmon resonance (SPR) analysis in UV-Vis spectrophotometer, while the size distribution was measured by a particle size analyzer. Surface morphology was performed using scanning electron microscopy (SEM), and antibacterial activity was evaluated by the disc diffusion method. The results showed that AgNPs had the best nanoparticle characteristics in an extract concentration of 0.5%, the synthesis indicated by SPR at a wavelength of 434 nm and an average size of 80.67 nm. SEM analysis showed the formation of clusters at variations of 1.0% and 1.5%. The antibacterial activity of AgNPs against MRSA was the highest at 0.5%, with an inhibition zone diameter of 0.77 mm. The higher concentration of *S. jamaicencis* leaf extract increases the risk of cluster formation, which enlarges the AgNPs, while antibacterial activity was reduced.

**KEYWORDS** Antibacteria; Biosynthesis; MRSA; Silver nanoparticles; *Stachytarpheta jamaicensis*

## 1. Introduction

Pathogenic microorganisms' resistant to antibiotics are a global threat to human health. In 2019, antibiotic-resistant bacteria caused at least 1.27 million deaths and are associated with approximately 5 million cases of infection worldwide (Murray et al. 2022). One of the resistant pathogen infections with high mortality and morbidity is the Methicillin-Resistant Staphylococcus aureus (MRSA) infection. The Asian region has the highest prevalence of MRSA infection worldwide, reaching 46–61% of infections (Ruekit et al. 2022).

There has been an increase in awareness of the spread of MRSA in the hospital environment due to its spread through direct contact between staff and patients as well as medical equipment, clothing, and the air. Erlin et al. (2020) found that there was exposure to MRSA on the instrument table (87%), surgical scissors (83%), bed sheets (67%), and infusion poles (75%) in the surgical treatment room. The spread of MRSA infection in hospitals can harm patient care by increasing morbidity and mortality and inflating treatment costs due to prolonged hospitalization duration and more expensive antimicrobial agents (Nkuwi et al. 2018). Effective antibacterial agents are needed to inhibit the spread of MRSA on tools and instruments in hospitals.

Silver nanoparticles have been widely developed as an antibacterial agent for coating polymer fibers and metal surfaces (Xia et al. 2018). Nanoscale metal nanoparticles (1–100 nm) can enlarge the antibacterial spectrum since they have a larger surface area per volume ratio (Rosman et al. 2021). Silver nanoparticles have multiple mechanisms of inhibiting bacteria growth, which may also be lethal, being able to attach or adhere to the surface of the bacterial membrane and change the structural integrity of the membrane (Lee and Jun 2019), entering cells and damaging their intracellular components, inducing the production of free radicals, and interfering the signaling transduction pathways on the bacterial life cycle (Yan et al. 2018).

Silver nanoparticles produced by physical and chemical methods require expensive reagents and production

systems utilizing hazardous conditions, that is high temperature and pressure, and longer processing time (Sardjono et al. 2022). Green synthesis is an alternative for the formation of silver nanoparticles by employing compounds contained in plants or microorganisms as natural reducing agents (bioreductant) to reduce silver metal ions (Jamkhande et al. 2019). Using extracts from natural ingredients makes green synthesis more environmentally friendly, has low production costs, and abundant raw materials in nature, allowing it to be produced on a larger scale (Sur et al. 2018).

Groups of plant metabolites such as flavonoids, phenolic, carbohydrates, sugars, and proteins act as reducing and stabilizing agents in the synthesis of AgNPs (Chahardoli et al. 2017). Plant secondary metabolites have polyhydroxy groups, which possess potent antioxidant activity and play a role in reducing metal ions into nanoparticles (Sahu et al. 2016). The hydroxyl group (-OH) in the flavonoid such as quercetin can be an ion reducing agent due to changes in the flavonoid tautomer from the enol to the keto-type, which releases reactive hydrogen atoms so that they can reduce silver ions into nanoparticles (Me et al. 2020).

*Stachytarpheta jamaicensis* is widely distributed in Indonesia and found in forest areas, meadows, gardens, and roadsides. The plant is used traditionally for healing allergies and digestive problems. Recent studies report that *S. jamaicensis* leaves contain flavonoids, tannins and saponins. These compounds have hydroxyl groups, so it can donate electrons to reduce Ag+ ions to nano-sized Ag0 (Yanuar et al. 2022).

Based on the potential of leaf extract as a bioreduction of silver nanoparticles, a study was conducted to characterize the biosynthesis of AgNPs with various extract concentrations. The concentration of the extract determines the effectiveness of reducing Ag+ ions thereby affecting the variations in shape, size and concentration of the AgNPs produced (Septriani and Muldarisnur 2022). Variations in shape, size, and concentration of the synthesized nanoparticles determine the antibacterial effectiveness of AgNPs (Dwiastuti et al. 2022). Therefore, this study aimed to determine the optimal concentration of precursors and plant extracts as bioreduction to produce AgNPs with the smallest size to inhibit the growth of MRSA.

## 2. Materials and Methods

### *2.1. Stachytarpheta jamaicensis leaf extract preparation*

The leaf *S. jamaicensis* was washed with water and air-dried. The dried leaf of *S. jamaicensis* was then crushed and filtered to a size of 20 mesh to form simplicia with a uniform size. The simplicia was extracted in 70% ethanol as a solvent at a ratio of 1:10 using an ultrasonic homogenizer (Biologics. Inc 150 v/t, USA) at a frequency of 20 kHz for 20 min. Then, the extract was filtered using filter paper to separate the filtrate and residue. The residue was then extracted again following the same method. The filtrate was then evaporated with a rotary evaporator (InScienPro EVA-700, Indonesia) at 60 °C until ¼ of the volume remained and then heated in a water bath at 60 °C to create a thick extract. The concentrated extract was subsequently diluted with distilled water to achieve concentrations of 0.5%, 1.0%, and 1.5%, thereby forming the test extract. The extraction process was conducted following the protocol of Abd Karim et al. (2022).

### *2.2. Biosynthesis of AgNPs with S. jamaicensis leaf extract*

The AgNPs biosynthesis process was carried out based on research conducted by Lestari et al. (2022) by modifying the addition of 1% poly vinyl alcohol (PVA). The concentrated extract was diluted to a concentration of 0.5%, 1.0%, and 1.5% to the test extract. The test extract for each concentration was added with 1 mM $AgNO_3$ with a volume ratio 1:10. Biosynthesis was evaluated in three repetitions for each concentration. The mixture was observed for changes in color and absorbance at 0, 24, and 48 h.

### *2.3. Characterization of AgNPs*

Several analyses have been carried out to characterize the prepared nanoparticles, as described in Du et al. (2022). The absorbance peak was determined using a UV-Vis spectrophotometer to determine the growth of nanoparticle formation. The absorbance peaks formed at specific wavelengths can be used to predict the formed nanoparticles' size and shape. The size and shape of the AgNPs supernatant were characterized and performed by a UV-Vis spectrophotometer (Hitachi UH5300, Japan) at a wavelength range of 350–800 nm.

#### 2.3.1 Surface plasmon resonance and absorbance analysis

The shape and size of AgNPs can be examined by UV-Vis spectrophotometer through surface plasmon resonance (SPR) analysis or an oscillatory resonance process due to the presence of an electromagnetic field from laser light with electrons on the surface of silver nanoparticles (Sarhan et al. 2022). SPR is a phenomenon that occurs when light interacts with tiny silver particles. When light as electromagnetic waves hit the surface of the nanoparticles, it will collectively cause the electrons on the surface to oscillate, creating a resonance effect (Lestari et al. 2022). The resonance effect can be detected through distinct wavelengths of light absorbed or scattered by the nanoparticles. Light absorption by particles in the UV-Vis spectrum depends on the electronic structure of the particles (Fazrin et al. 2020).

Nanoparticle suspension is vortex gently to ensure uniform dispersion. For optimal results, we use freshly prepared and well-dispersed samples. For blank preparation, a clean cuvette was filled with deionized water. The blank cuvette was inserted into the spectrophotometer and run a

baseline correction which set the instrument to zero. Next, a 1 mL volume of the nanoparticle suspension was transferred into a clean cuvette and inserted the sample cuvette into the UV-Vis spectrophotometer. The absorbance of the synthesized AgNPs solution was measured at each concentration over intervals of 0, 24, and 48 hours to observe the rate of AgNPs formation. The wavelength was recorded within the range of 350–800 nm, and the peak wavelength was subsequently identified. For silver nanoparticles, a peak is typically observed near 400 nm.

Identifying the surface plasmon resonance (SPR) peak is essential for data interpretation, as its position is related to particle size and dispersion state. A red shift, where the peak moves to longer wavelengths, indicates larger particles or aggregation. In contrast, a blue shift, where the peak shifts to shorter wavelengths, suggests smaller particles or surface modifications. Additionally, it is important to measure the peak intensity since it correlates with particle concentration. The full width at half maximum (FWHM) should also be evaluated to determine the size distribution of nanoparticles; broader peaks indicate greater size variability or aggregation among the particles. The measurements are repeated at least three times to ensure the reliability of the data.

#### 2.3.2 Particle size analysis

The size distribution of AgNPs is based on diameter, polydispersity index, and Z average parameters, which can be analyzed by a particle size analyzer (PSA) device. PSA is an instrument that can measure particle size distribution in emulsions, suspensions, and dry powders. The advantage of this instrument is that it has an accuracy of ± 1% and can measure particles from 0.2 nm to 2,000 nm. PSA analysis can confirm the particle size and distribution of the nanoparticles formed in the presumed SPR (Ulayya et al. 2019). Confirmation of nanoparticle size was performed using a size distribution analysis device (Horiba SZ-100, Japan). Size distribution analysis used AgNPs supernatant purified of the synthesis solution by centrifugation (Eppendorf centrifuge 5810R) of all concentrations at 1500 rpm for 10 min. A volume of 1 mL of the sample solution was transferred into the cuvette and subsequently placed in the holder of the PSA machine. The PSA device provided the polydispersity index parameters and the nanoparticles' average size.

#### 2.3.3 Scanning electron microscopy (SEM) analysis

SEM analysis produces surface morphological structure images of silver nanoparticles. SEM is an electron microscope that depicts the sample's surface through scanning from high-emission electrons (Hutagalung et al. 2022). The surface morphology of AgNPs describe the shape of the particles and the shape of the clusters formed. The estimated shape and size of nanoparticles by SPR analysis can be confirmed utilizing SEM devices. SEM is a method that can directly characterize the microscopic morphology of AgNPs (Du et al. 2022). The morphology of the silver nanoparticles was confirmed by an SEM device (Thermo FEI Quanta 250, USA). Morphological analysis was performed on 20 µl of AgNPs supernatant dripped onto the fiber (0.6 mm diameter) with 5 µl 1% PVA as fixative nanoparticle media and allowed to dry. The fiber was then analyzed with an SEM device at 50,000× optical magnification.

### 2.4. Antibacterial activity test

The disc diffusion method was used to test the antibacterial activity of AgNPs toward MRSA on Mueller Hinton Agar (MHA) media. MRSA was obtained from the Faculty of Medicine, Sebelas Maret University. The tested MRSA was refreshed by subculture on Nutrient Agar (NA) and incubated at 37 °C overnight. The MRSA culture was subsequently suspended in 0.95% physiological saline to achieve a turbidity level equivalent to 0.5 McFarland. It was then uniformly spread on the surface of the MHA medium using a sterile cotton swab. McFarland standards are used to standardize the approximate number of bacteria in a liquid suspension by comparing the turbidity of the sample. These standards range from 0.5 to 10, with each standard representing a specific bacterial concentration. A 0.5 McFarland standard corresponds to approximately $1.5\times10^8$ colony-forming units per milliliter (CFU/mL), which meets the required bacterial count for the antimicrobial susceptibility testing (Aryal 2021). Five paper discs were placed on the media and then dripped with AgNPs supernatant (30 µL), ciprofloxacin 32 µg/mL as a positive control, aquadest as a negative control, and the treatments *S. jamaicensis* leaf extract and 1mM $AgNO_3$ each as much as 5 µL. In several studies on MRSA, ciprofloxacin at a concentration of 32 µg/mL was used as a reference in antimicrobial activity tests. This concentration reflects a high level of exposure necessary to overcome bacterial resistance, particularly in more challenging strains like MRSA (Kang et al. 2020). Only 5 µL of the synthesized AgNPs were utilized, as previous research indicated that this volume was the minimum required to demonstrate antibacterial activity and to ensure optimal absorption by the paper disk (Devanesan and Alsalhi 2021). The cultures were incubated for 24 h at 37 °C. Each treatment was carried out in three replicates. Antibacterial activity testing was conducted qualitatively, following the procedur of Indah et al. (2022).

### 2.5. Data analysis

Qualitative data for the characteristics of AgNPs, including absorbance, particle size, distribution index, and antibacterial activity in the form of inhibition zone diameter, were analyzed descriptively.

## 3. Results and Discussion

### 3.1. Ethanolic extract of Stachytarpheta jamaicensis leaf

*S. jamaicensis* leaf extract was produced by dissolving 48.2 g of *S. jamaicensis* leaf simplicia in 482 mL of 70% ethanol and producing a thick extract of 18.1 g. The yield percentage based on the ratio of the viscous extract's weight to the sample's weight showed a percentage of 37.67% (Table 1).

The percentage of yield obtained is more than 30%, which means the extraction process has been running optimally. Based on the standardization of the (Directorate General of Food and Drug Administration 2000), optimally, the extraction process occurs when it reaches more than 10%. The yield with a high percentage showed the type of solvent and extraction method optimally dissolved the content of *S. jamaicensis* metabolites. Ethanol at a concentration of 70% as a solvent has been reported to produce more plant extract yields as it has a higher polarity than at higher concentrations (Suhendra et al. 2019). Ethanol solvents can dissolve metabolites by degrading cell walls and dissolving the bioactive compounds of plant cells with the ethanol hydroxyl group bonded to the hydrogen group of the hydroxyl group of phenolic compounds.

**TABLE 1** Percentage of the yield of *S. jamaicensis* leaf extraction with 70% ethanol as a solvent using the sonication method for 20 minutes.

| Sample Weight (g) | Solvent Volume (mL) | Extract Weight (g) | Yield Percentage (%) |
|---|---|---|---|
| 48.2 | 482 | 18.1 | 37.67 |

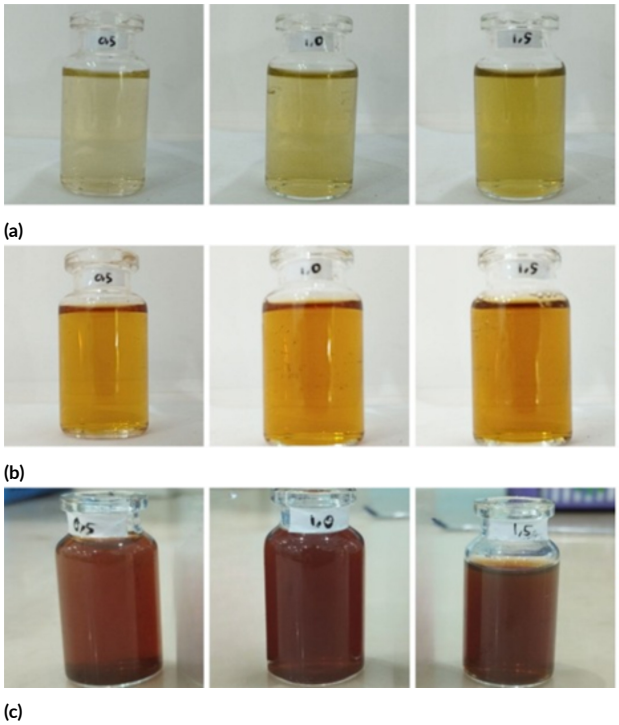


**FIGURE 1** The color of the silver nanoparticle synthesis solution with various concentrations of S. jamaicensis leaf extract (0.5%, 1.0%, and 1.5%) at (a) 0 hours, (b) 24 hours, and (c) 48 hours.

The sonication method was used since it requires a relatively short time and a smaller amount of solvent than other extraction methods (Jumawardi et al. 2021). Sonication can increase the frequency and area of cell surface contact with the solvent to streamline the time and amount of solvent used (Xu et al. 2021). In addition to this, the reducing compounds contained in *S. jamaicensis* leaves, including antioxidants, phenolic, flavonoids, tannins, and saponins, which are thermolabile, make sonication an appropriate extraction method (Oprescu et al. 2022).

### 3.2. Biosynthesis of silver nanoparticle

The process of biosynthesis of silver nanoparticles can be observed directly. Visual observation was carried out by observing changes in the turbidity and color of the synthesis solution. Increased turbidity and color change of the synthesis solution can indicate the process of forming silver nanoparticles. One mM precursor $AgNO_3$ was reacted with *S. jamaicensis* leaf extract (0.5%, 1.0%, and 1.5%) to produce a clear yellowish solution, which became more intense over time. The color change of the silver nanoparticle synthesis solution at 0, 24, and 48 hours is shown in Figure 1.

The color of the synthesis solution that is darkened with time indicates an increase in particle size and the presence of surface plasmonic effects (Fazrin et al. 2020). The plasmonic effect is when light interacts with electrons on the surface of small particles. When it reaches the particle's surface, light energy can generate plasmonic waves. Plasmonic vibrations are the collective vibrations of the electrons on the particle's surface. When AgNP particles are formed, they produce a specific shape and size that produce a distinctive plasmonic effect. The plasmon waves that are formed can create electromagnetic resonance at specific wavelengths. These resonances can affect silver nanoparticles to absorb and reflect light waves. Larger AgNP particles absorb more light at shorter wavelengths, including visible light, and reflect light at longer wavelengths. As a result, larger AgNPs tend to have a darker or more brownish color (Amaliyah et al. 2022).

Changes in turbidity and the color of the synthesis solution to dark brown simultaneously indicate that the biosynthesis rate has reached the final phase. The clustering process of the biosynthesis of silver nanoparticles with reducing agents of plant bioactive compounds occurs in three phases: induction, growth, and termination. The induction phase initiates the synthesis process by reducing silver ions and nucleating them into small, reactive, and unstable crystals. These ions then spontaneously aggregate into larger aggregates, indicating a growth phase. In the termination phase, the size and shape of the biomolecule-enclosed aggregate as a capping agent.

### 3.3. Absorbance response and peak wavelength of silver nanoparticles (AgNPs)

The biosynthesis of silver nanoparticles can be determined based on surface plasmon resonance (SPR) and absorbance analysis. Visual observation of the silver nanoparticle synthesis solution was strengthened by measuring the absorbance spectrum applied in a UV-Vis spectrophotometer over time during biosynthesis. The peak wavelength of the nanoparticles from all variations in concentrations of *S. jamaicensis* leaf was formed in the 429–436 nm (Table 2). The peak wavelength is the SPR of the formed nanoparticles. SPR at that wavelength range shows biosynthesis at each concentration variation to produce nanometer-sized AgNPs. SPR at this wavelength range is following previous studies that reported silver nanoparticles could be identified by the SPR phenomenon at a wavelength of 400–450 nm (Eid et al. 2020).

The 24-hour biosynthesis time showed that biosynthesis with higher concentrations of *S. jamaicensis* leaves produced SPR at shorter wavelengths. SPR that shifts to shorter wavelengths also shows smaller particle sizes (Septriani and Muldarisnur 2022). These results state that using *S. jamaicensis* leaf extract as a reducing agent in higher concentrations forms smaller-sized nanoparticles.

The biosynthesis time at 48 hours showed that at a concentration of 1.5%, the SPR shift was longer than the other concentration variations. The move of the absorption peak to longer wavelengths indicates that the stability of silver nanoparticles is less stable and tends to experience agglomeration (Prasetyaningtyas et al. 2020). In addition, there was a significant increase in absorbance at a concentration of 1.5% compared to other concentrations (Figure 2).

The increased absorbance intensity represents an accumulation in the reduction of silver ions to silver atoms, resulting in an increase in the formed nanoparticle concentration. Raising the concentration of nanoparticles results in a more likely tension force for silver to occur, which causes the size of the silver nanoparticles to be larger due to the formation of clusters.

### 3.4. Size distribution of silver nanoparticle

The supernatant from the synthesis solution at 48 h of synthesis time, which was centrifuged at 1500 rpm for 10 min, was characterized by a particle size analyzer (PSA). The value of the polydispersity index (Pd.i) and the average Z value can be seen in Table 3.

Table 3 shows that the average size of the nanoparticles (Z average) and the diameter (d.nm) increased by elevating the concentration of *S. jamaicensis* leaf extract used. The average size of the smallest nanoparticles, i.e. 80.67 nm, was obtained in the synthesis of 0.5% extract, and the average size of the largest nanoparticles was found in the synthesis of 1.5% extract, which was 111.2 nm. This shows that a 0.5% concentration of *S. jamaicensis* leaf extract allows the provision of sufficient antioxidants and other bioreduction compounds to synthesize silver nanoparticles with an acceptable size. If the concentration of the extract is excessive, it can cause the reaction to continue and enlarge in size.

The size distribution curve can be seen in Figure 3. The curve in Figure 3 has peaks that indicate the size distribution of AgNPs. The peak on the distribution curve designates that AgNPs of all concentration variations have the highest particle size frequency below 100 nm. However, the concentration of 1.5% has particles with sizes above 100 nm in a higher percentage than the other variations.

PSA analysis presented that all silver nanoparticles

**TABLE 2** Peak wavelength and absorbance of silver nanoparticles based on biosynthesis time.

| Concentration | 0th hour | | 24th hour | | 48th hour | |
|---|---|---|---|---|---|---|
| (%) | Wavelength (nm) | Absorbance | Wavelength (nm) | Absorbance | Wavelength (nm) | Absorbance |
| 0.5 | 676 | 0.047 | 436 | 0.974 | 434 | 1.002 |
| 1 | 676.5 | 0.084 | 431.5 | 1.321 | 430 | 1.469 |
| 1.5 | 674.5 | 0.111 | 429.5 | 1.36 | 430 | 2.55 |

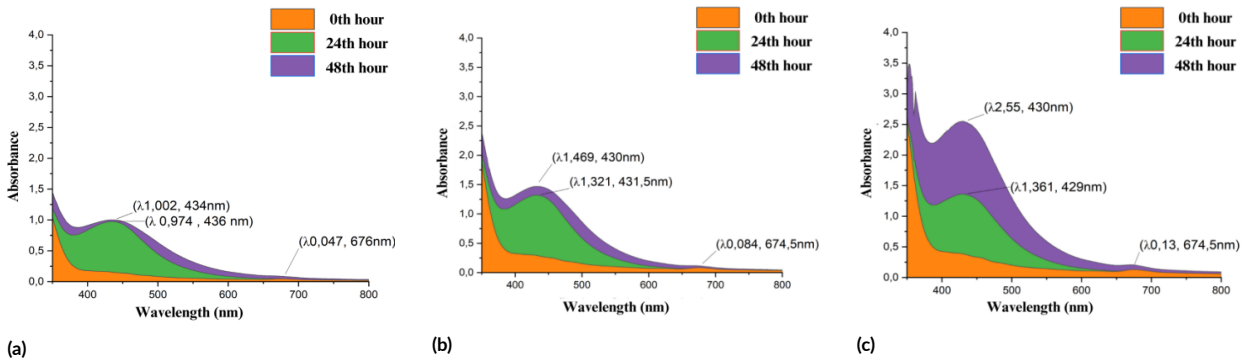


**FIGURE 2** Peak wavelength and absorbance: (a) 0.5% extract, (b) 1.0% extract, and (c) 1.5% extract. It was observed that there was a shift in the absorption peak at the 48th hour of synthesis and an increase in absorbance in the 1.5% variation of the extract.

**TABLE 3** Diameter size of nanoparticles, polydispersity index, and average size of silver nanoparticles formed.

| Extract concentration (%) | Diameter Size (d.nm) | Pd. Index | Z Average (nm) |
|---|---|---|---|
| 0.5 | 43.67 | 0.256 | 80.67 |
| 1 | 43.49 | 0.36 | 89.68 |
| 1.5 | 63.54 | 0.311 | 111.2 |

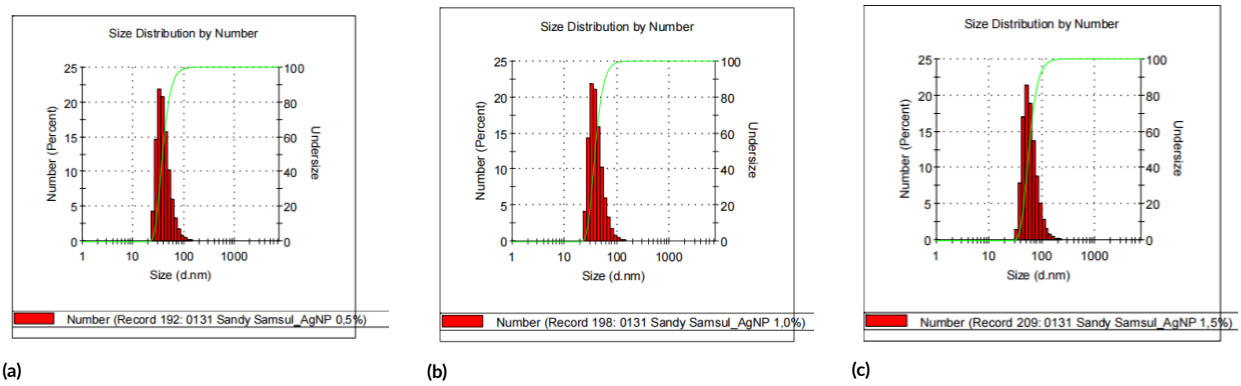


(a) (b) (c)

**FIGURE 3** Size distribution curve from particle size analyzer: (a) Silver nanoparticles with 0.5% extract with a peak below 100 nm, (b) 1.0% with a peak below 100 nm, (c) 1.5 with a peak below 100 nm, but some curves exceed 100 nm.

with various concentrations of extracts had a reasonable degree of homogeneity in particle size. The polydispersity index value of the three variations shows a value below 0.5, which denotes good uniformity of the size of the nanoparticles (Amiri and Behin 2021). The smaller the polydispersity index value, the more homogeneous the particle size. Meanwhile, if the polydispersity index value of the nanoparticles exceeds 0.5, the size of the nanoparticles is heterogeneous (Lestari et al. 2022).

### *3.5. Surface morphology of silver nanoparticles*

Scanning electron microscopy (SEM) is an instrument in the form of an electron microscope that can image the sample surface by scanning from the electron beam. SEM emits an electron beam, which will be reflected by the particles to be captured by the detector and analyzed to initiate an image (Hutagalung et al. 2022). Morphological observations were carried out at magnifications of 50,000×. The surface morphology of AgNPs at 50,000× magnification can be seen in Figure 4.

Surface morphology images of AgNPs show the biosynthesis of silver nanoparticles of all concentration variations having sizes below one µm. Morphologically, from SEM observations, nanoparticles have formed with the observed surface shaped like small spheres. The silver nanoparticles biosynthesized from the 0.5% extract revealed spherical nanoparticles sticking together. SEM images at 1.0% and 1.5% variations demonstrate that the nanoparticles agglomerate with each other to form large clusters covering the pores of the filter paper.

Several driving factors can cause the formation of silver nanoparticle clusters. The higher the extract concentration as a reducing agent, the higher the nanoparticle concentration formed relatively quickly. The high concentration of nanoparticles formed generates a tendency for nanoparticles to experience agglomeration due to Van der Waals forces (Lestari et al. 2022). Silver nanoparticles that undergo agglomeration have a low zeta potential value due to the attraction between nanoparticles, which is greater than the repulsive force between them. Low zeta potential

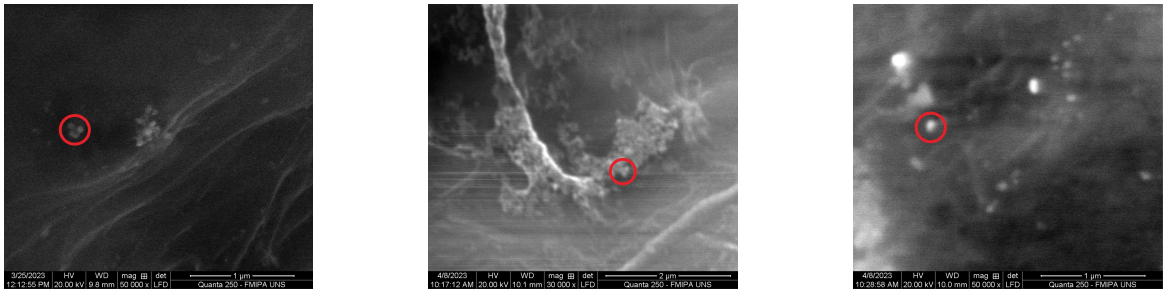

(a) (b) (c)

**FIGURE 4** Scanning Electron Microscopy (SEM) image of surface morphology of silver nanoparticles at 50,000× magnification on filter paper pores, (a, b, c) silver nanoparticles extract 0.5%, 1.0%, and 1.5% respectively. Note: red circle indicates AgNPs.

values specify silver nanoparticles that are less stable and experience agglomeration.

### *3.6. Antibacterial activity of silver nanoparticle*

Silver nanoparticles with a 48-hour biosynthesis time, which have been identified to form nanoparticles, were then tested for their antibacterial activity. Figure 5 shows the inhibition zone of antibacterial activity.

Table 4 reveals the diameter of the silver nanoparticle inhibition zone against MRSA. Silver nanoparticles of each variation showed a diameter of inhibition on the growth of MRSA. AgNP variation of 0.5% extract produced the widest diameter of the inhibition zone, which gave better antibacterial effectiveness than the other variations. The diameter of the inhibition zone is consistent with the size of the silver nanoparticles; the smaller the size of the silver nanoparticles, the wider the diameter of the inhibition. Previous reports explained that nanoparticle size can affect antibacterial effectiveness since it is related to the ratio of surface area to particle volume. The smaller the particle size, the easier it is for silver nanoparticles to penetrate the bacterial cell wall to change the cell membrane's structure and trigger cell death (Yin et al. 2020). Research by Alavi et al. (2019) proved that silver nanoparticles can enter the cell membrane of *S. aureus* bacteria, leading to changes in cell morphology to swell and shrink due to shrinking cell walls.

AgNPs is widely used as an antibacterial agent, exhibiting various inhibitory mechanisms in bacteria. AgNPs can attach (adhesion) directly to the bacterial cell membrane due to differences in electrostatic charge (Lee and Jun 2019). Furthermore, AgNPs will cause holes in the membrane, causing the membrane to fail to protect intracellular organs, resulting in cell death (Masimen et al. 2022). The existence of a hole due to changes in the permeability and structural integrity of the membrane attached to AgNPs causes AgNPs to enter the cell (Hochvaldová et al. 2022). AgNPs then interacts with cellular molecules and organelles such as proteins, DNA, and lipids. AgNPs, which interacts with the ribosome, will interfere with protein synthesis by denaturing the ribosome and stopping the translation process (Mateo and Jiménez 2022). AgNPs can also bind with DNA molecules, contributing to DNA denaturation and cutting, as well as disruption of cell division. The interaction of cell cellular organelles with AgNPs causes bacteria to lose their ability to divide or reproduce, which ends in cell death (Masimen et al. 2022). AgNPs will release Ag+ ions, which induce high levels of reactive oxygen species (ROS), causing cell oxidative stress (Yan et al. 2018). Oxidative stress can cause damage to vital cellular organelles such as proteins, DNA, and RNA.

**TABLE 4** Diameter of the AgNPs inhibition zone in MRSA bacteria culture.

| Treatment | Inhibition zone diameter (mm) |
|---|---|
| AgNPs Variation 0.5% | 1.37 |
| AgNPs Variation 1.0% | 0.85 |
| AgNPs Variation 1.5% | 0.75 |
| $AgNO_3$ | 0.73 |
| Extract 1.5% | 0 |
| Aquades (negative control) | 0 |
| Ciprofloxacin (positive control) | 19.65 |

AgNPs treatment at all variations concentration demonstrated an inhibition zone, albeit minimal when compared to the positive control ciprofloxacin. Several factors could contribute to this observation, such as the low nanoparticle concentration and the types of bacteria tested. This highlights the importance of purifying AgNPs produced through biosynthesis, as this research relied solely on the volume of supernatant. Purifying AgNPs eliminates biosynthesis residues and excess bioactive components, like flavonoids and enzymes from plant extracts, which can influence measurements of nanoparticle concentrations. Therefore, more consistent quantification of AgNPs can be achieved, ensuring that the concentrations used in antibacterial assays are both precise and reproducible (Nkosi et al. 2024).

According to previous studies (Amaliyah et al. 2022; Alavi et al. 2019; Hasanzadeh et al. 2021), silver nanoparticles produce smaller inhibition zones in gram-positive bacteria such as *Staphylococcus aureus* than in Gram-

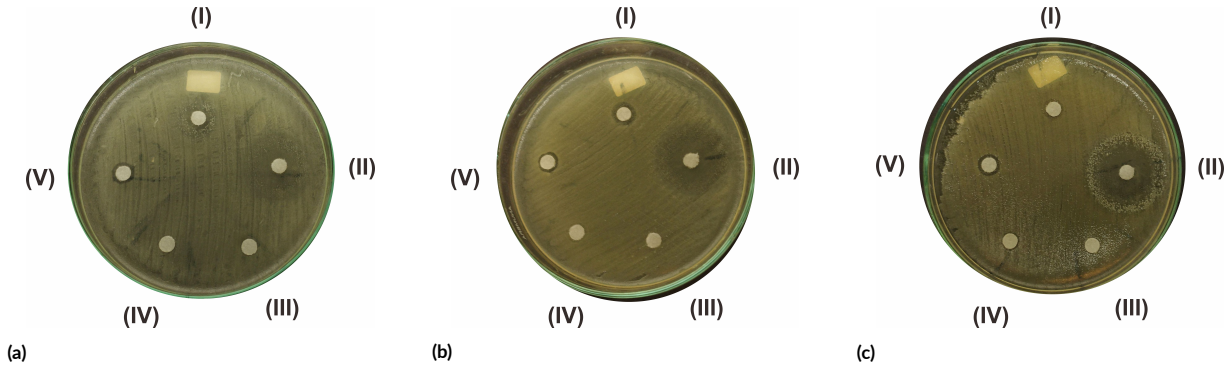


**FIGURE 5** Inhibition zone of silver nanoparticles (I) AgNPs ((a) 0.5 %, (b) 1.0%, (c) 1.5%)), (II) ciprofloxacin, (III) Extract, (IV) Aquadest, and (V) $AgNO_3$.

negative bacteria such as *Escherichia coli*. Amaliyah et al. (2022), using *Piper retrofractum* (Javanese chili) fruit extract as a reducing agent, reported inhibition zones for *S. aureus* around 12–16 mm, while for *E. coli* it reached 18–20 mm (include paper disk diameter 6 mm), suggesting higher sensitivity of Gram-negative bacteria in this case. Alavi et al. (2019) utilized the herbal extract *Pelargonium graveolens* (geranium) and found inhibition zones for *S. aureus* at 10–15 mm, while Gram-negative strains like *Pseudomonas aeruginosa* reached 17–22 mm. Hasanzadeh et al. (2021), employed *Mentha piperita* (peppermint) leaf extract, documented *S. aureus* inhibition zones around 14 mm, with *E. coli* showing zones up to 21 mm. The difference in the effect of AgNPs on Gram-positive and Gram-negative bacteria may be due to differences in the membrane structure's characteristics and the nanoparticles' nature and size.

Recent studies show that silver nanoparticles (AgNPs) with ideal size and shape might still exhibit suboptimal antibacterial performance. One explanation is that while the morphology and stability of the AgNPs contribute to their potential activity, other factors, such as the interaction with biological environments, agglomeration, or insufficient surface reactivity, can hinder their effectiveness. For example, a 2022 fungal-mediated synthesis study produced well-characterized, stable, and spherical AgNPs. Despite their excellent physical properties, the antibacterial inhibition zones varied significantly depending on the bacterial strain. The interaction between AgNPs and bacterial membranes can be affected by the nanoparticle's surface chemistry, capping agents, and environmental conditions, which might reduce their bioavailability or prevent them from releasing sufficient silver ions for optimal inhibition activity (Murillo-Rábago et al. 2022).

Furthermore, AgNPs synthesized with organic or inorganic carriers may exhibit lower antibacterial activity than expected. In these cases, the support material can limit the release of silver ions or the AgNPs may be sterically hindered from interacting efficiently with bacterial cells (Cacaci et al. 2023). Thus, while synthesis methods may produce AgNPs with ideal size and shape, their antibacterial performance depends on a complex interplay of physicochemical properties and environmental factors.

## 4. Conclusions

It was concluded that the concentration of *S. jamaicensis* leaf extract produced different characteristics of NPAg including SPR (0.5%: 434 nm, 1.0%: 430 nm, 1.5%: 430 nm), Z Average size distribution (0.5%: 80.67 nm, 1.0%: 89.68 nm, 1.5%: 111.2 nm), and surface morphology (0.5%: spheres stuck together, 1.0%: clusters, 1.5%: clusters). Based on this, a concentration of 0.5% produced the best NPAg character. The highest antibacterial activity of NPAg against MRSA bacteria was in 0.5% *S. jamaicensis* leaf extract with an inhibition zone of 0.77 mm, followed by 1.0% and 1.5%, respectively 0.25 mm wide and 0.15 mm. The higher concentration of *S. jamaicensis* leaf extract used increases the risk of cluster formation, which makes the size of the AgNPs enlarge and the antibacterial activity decrease.

## Acknowledgments

This research was partially funded by non-APBN funds 2023, through the Research Group Grant, Sebelas Maret University.

## Authors' contributions

Designed the experiments SSB, AS, AP, Performing research: SSB. Analyzed the data: SSB, AS, AP. Wrote the paper: SSB, AS, AP.

## Competing interests

All authors have examined the manuscript and declare no competing interests.

## References

Abd Karim F, Tungadi R, Thomas NA. 2022. Biosintesis nanopartikel perak ekstrak etanol 96% daun kelor (*Moringa oleifera*) dan uji aktivitasnya sebagai antioksidan [Biosynthesis of silver nanoparticles from ethanol extract of 96% Moringa leaves (*Moringa oleifera*) and testing its activity as an antioxidant]. Indones. J. Pharm. Educ. 2(1):32–41. doi:10.37311/ijpe.v2i1.11725.

Alavi M, Karimi N, Valadbeigi T. 2019. Antibacterial, antibiofilm, antiquorum sensing, antimotility, and antioxidant activities of green fabricated Ag, Cu, $TiO_2$, ZnO, and $Fe_3O_4$ NPs via *Protoparmeliopsis muralis* lichen aqueous extract against multi-drug-resistant bacteria. ACS Biomater. Sci. Eng. 5(9):4228–4243. doi:10.1021/acsbiomaterials.9b00274.

Amaliyah S, Sabarudin A, Masruri M, Sumitro SB. 2022. Characterization and antibacterial application of biosynthesized silver nanoparticles using *Piper retrofractum* Vahl fruit extract as bioreductor. J. Appl. Pharm. Sci. 12(3):103–114. doi:10.7324/JAPS.2022.120311.

Amiri P, Behin J. 2021. Assessment of aqueous phase ozonation on aggregation of polyvinylpyrrolidone-capped silver nanoparticles. Environ. Sci. Pollut. Res. 28(26):34838–34851. doi:10.1007/s11356-021-12475-y.

Aryal S. 2021. Mc Farland Standarts-Principle, Preparation, Uses, Limitations. Microbe Notes. URL https://microbenotes.com/mcfarland-standards/.

Cacaci M, Biagiotti G, Toniolo G, Albino M, Sangregorio C, Severi M, Di Vito M, Squitieri D, Contiero L, Paggi M, Marelli M, Cicchi S, Bugli F, Richichi B. 2023. Shaping silver nanoparticles' size through the carrier composition: Synthesis and

antimicrobial activity. Nanomaterials 13(10):1585. doi:10.3390/nano13101585.

Chahardoli A, Karimi N, Fattahi A. 2017. Biosynthesis, characterization, antimicrobial and cytotoxic effects of silver nanoparticles using *Nigella arvensis* seed extract. Iran. J. Pharm. Res. 16(3):1167.

Devanesan S, Alsalhi MS. 2021. Green synthesis of silver nanoparticles using the flower extract of *Abelmoschus esculentus* for cytotoxicity and antimicrobial studies. Int. J. Nanomedicine 16:3343–3356. doi:10.2147/IJN.S307676.

Directorate General of Food and Drug Administration. 2000. Parameter Standar Umum Ekstrak Tumbuhan Obat. Departemen Kesehatan Republik Indonesia [General Standard Parameters of Medicinal Plant Extracts]. Jakarta: Indonesian Ministry of Health.

Du P, Xu Y, Shi Y, Xu Q, Li S, Gao M. 2022. Preparation and shape change of silver nanoparticles (Ag-NPs) loaded on the dialdehyde cellulose by in-situ synthesis method. Cellulose 29(12):6831–6843. doi:10.1007/s10570-022-04692-6.

Dwiastuti R, Suhendra PA, Yuliani SH, Riswanto FDO. 2022. Application of the central composite design approach for optimization of the nanosilver formula using a natural bioreductor from *Camellia sinensis* L. extract. J. Appl. Pharm. Sci. 12(8):048–056. doi:10.7324/JAPS.2022.120806.

Eid AM, Fouda A, Niedbała G, Hassan SED, Salem SS, Abdo AM, Hetta HF, Shaheen TI. 2020. Endophytic *Streptomyces laurentii* mediated green synthesis of Ag-NPs with antibacterial and anticancer properties for developing functional textile fabric properties. Antibiotics 9(10):641. doi:10.3390/antibiotics9100641.

Erlin E, Rahmat A, Redjeki S, Purwianingsih W. 2020. Deteksi methicilin resistant *Staphylococcus aureus* (MRSA) sebagai penyebab infeksi nosokomial pada alat-alat di ruang perawatan bedah [Detection of methicillin resistant *Staphylococcus aureus* (MRSA) as a cause of nosocomial infections in instruments in the surgical treatment room]. Quagga J. Pendidik. dan Biol. 12(2):137–144. doi:10.25134/quagga.v12i2.2671.

Fazrin EI, Naviardianti AI, Wyantuti S, Gaffar S, Hartati YW. 2020. Review: Sintesis dan karakterisasi nanopartikel emas (AuNP) serta konjugasi AuNPs dengan DNA dalam aplikasi biosensor elektrokimia [Review: Synthesis and characterization of gold nanoparticles (AuNP) and conjugation of AuNPs with DNA in electrochemical biosensor applications]. PENDIPA J. Sci. Educ. 4(2):21–39. doi:10.33369/pendipa.4.2.21-39.

Hasanzadeh A, Gholipour B, Rostamnia S, Eftekhari A, Tanomand A, Valizadeh K A, Khaksar S, Khalilov R. 2021. Biosynthesis of AgNPs onto the urea-based periodic mesoporous organosilica (AgxNPs/Ur-PMO) for antibacterial and cell viability assay. J. Colloid Interface Sci. 585:676–683. doi:10.1016/j.jcis.2020.10.047.

Hochvaldová L, Večeřová R, Kolář M, Prucek R, Kvítek L, Lapčík L, Panáček A. 2022. Antibacterial nanomaterials: Upcoming hope to overcome antibiotic resistance crisis. Nanotechnol. Rev. 11(1):1115–1142. doi:10.1515/ntrev-2022-0059.

Hutagalung R, Permana AP, Isa DR. 2022. Kajian pelapukan granit Daerah Leato berdasarkan analisis XRD dan SEM [Granite weathering study in Leato Area based on XRD and SEM analysis]. EnviroScienteae 18(1):38–43. doi:10.20527/es.v18i1.12977.

Indah, Asri M, Auliah N, Ashari AT. 2022. Sintesis nanopartikel perak dengan air rebusan daun Pegagan (*Centella asiatica* L.) dan uji aktivitas dalam menghambat pertumbuhan bakteri *Pseudomonas aeruginosa* dan *Staphylococcus aureus* [Synthesis of silver nanoparticles with boiled water of Gotu Kola leaves (*Centella asiatica* L.) and activity test in inhibiting the growth of *Pseudomonas aeruginosa* and *Staphylococcus aureus* bacteria]. Majalah Farmasi dan Farmakologi 26(2):88–91.

Jamkhande PG, Ghule NW, Bamer AH, Kalaskar MG. 2019. Metal nanoparticles synthesis: An overview on methods of preparation, advantages and disadvantages, and applications. J. Drug Deliv. Sci. Technol. 53:101174. doi:10.1016/j.jddst.2019.101174.

Jumawardi R, Ananto AD, Deccati RF. 2021. Aktivitas antioksidan ekstrak etanol daun pecut kuda (*Stachytarpheta jamaicensis* (L.) Vahl) menggunakan metode ekstraksi berbasis gelombang ultrasonic [Antioxidant activity of ethanol extract of horsetail leaves (*Stachytarpheta jamaicensis* (L.) Vahl) using ultrasonic wave-based extraction method]. Sasambo J. Pharm. 2(2):80–86. doi:10.29303/sjp.v2i2.85.

Kang S, Sunwoo K, Jung Y, Hur JK, Park KH, Kim JS, Kim D. 2020. Membrane-targeting triphenylphosphonium functionalized ciprofloxacin for methicillin-resistant *Staphylococcus aureus* (MRSA). Antibiotics 9(11):758. doi:10.3390/antibiotics9110758.

Lee SH, Jun BH. 2019. Silver nanoparticles: Synthesis and application for nanomedicine. Int. J. Mol. Sci. 20(4):865–870. doi:10.3390/ijms20040865.

Lestari GAD, Ratnasari PMD, Sibarani J. 2022. Aplikasi antibakteri nanopartikel perak (NPAg) hasil biosintesis dengan ekstrak air daun kemangi [Antibacterial application of silver nanoparticles (NPAg) biosynthesized with basil leaf water extract]. KOVALEN J. Ris. Kim. 8(1):17–24. doi:10.22487/kovalen.2022.v8.i1.15771.

Masimen MAA, Harun NA, Maulidiani M, Ismail WIW. 2022. Overcoming methicillin-resistance *Staphylococcus aureus* (MRSA) using antimicrobial peptides-silver nanoparticles. Antibiotics 11(7):951. doi:10.3390/antibiotics11070951.

Mateo EM, Jiménez M. 2022. Silver nanoparticle-based therapy: Can it be useful to combat multidrug resistant bacteria? Antibiotics 11(9):1205.

doi:10.3390/antibiotics11091205.

Me R, Istamam MH, Amir NAS, Iberahim R, Shanthi A, Pungot NH, Ibrahim N. 2020. Role of Plant's metabolites in the biomimetic synthesis of plant-mediated silver nanoparticles: A review. Asian J. Fundam. Appl. Sci. 1(4):1–9.

Murillo-Rábago EI, Vilchis-Nestor AR, Juarez-Moreno K, Garcia-Marin LE, Quester K, Castro-Longoria E. 2022. Optimized synthesis of small and stable silver nanoparticles using intracellular and extracellular components of fungi: An alternative for bacterial inhibition. Antibiotics 11(6):800. doi:10.3390/antibiotics11060800.

Murray CJ, Ikuta KS, Sharara F, Swetschinski L, Robles Aguilar G, Gray A, Han C, Bisignano C, Rao P, Wool E, Johnson SC, Browne AJ, Chipeta MG, Fell F, Hackett S, Haines-Woodhouse G, Kashef Hamadani BH, Kumaran EA, McManigal B, Agarwal R, Akech S, Albertson S, Amuasi J, Andrews J, Aravkin A, Ashley E, Bailey F, Baker S, Basnyat B, Bekker A, Bender R, Bethou A, Bielicki J, Boonkasidecha S, Bukosia J, Carvalheiro C, Castañeda-Orjuela C, Chansamouth V, Chaurasia S, Chiurchiù S, Chowdhury F, Cook AJ, Cooper B, Cressey TR, Criollo-Mora E, Cunningham M, Darboe S, Day NP, De Luca M, Dokova K, Dramowski A, Dunachie SJ, Eckmanns T, Eibach D, Emami A, Feasey N, Fisher-Pearson N, Forrest K, Garrett D, Gastmeier P, Giref AZ, Greer RC, Gupta V, Haller S, Haselbeck A, Hay SI, Holm M, Hopkins S, Iregbu KC, Jacobs J, Jarovsky D, Javanmardi F, Khorana M, Kissoon N, Kobeissi E, Kostyanev T, Krapp F, Krumkamp R, Kumar A, Kyu HH, Lim C, Limmathurotsakul D, Loftus MJ, Lunn M, Ma J, Mturi N, Munera-Huertas T, Musicha P, Mussi-Pinhata MM, Nakamura T, Nanavati R, Nangia S, Newton P, Ngoun C, Novotney A, Nwakanma D, Obiero CW, Olivas-Martinez A, Olliaro P, Ooko E, Ortiz-Brizuela E, Peleg AY, Perrone C, Plakkal N, Ponce-de Leon A, Raad M, Ramdin T, Riddell A, Roberts T, Robotham JV, Roca A, Rudd KE, Russell N, Schnall J, Scott JAG, Shivamallappa M, Sifuentes-Osornio J, Steenkeste N, Stewardson AJ, Stoeva T, Tasak N, Thaiprakong A, Thwaites G, Turner C, Turner P, van Doorn HR, Velaphi S, Vongpradith A, Vu H, Walsh T, Waner S, Wangrangsimakul T, Wozniak T, Zheng P, Sartorius B, Lopez AD, Stergachis A, Moore C, Dolecek C, Naghavi M. 2022. Global burden of bacterial antimicrobial resistance in 2019: A systematic analysis. Lancet 399(10325):629–655. doi:10.1016/S0140-6736(21)02724-0.

Nkosi NC, Basson AK, Ntombela ZG, Dlamini NG, Pullabhotla RVSR. 2024. Green synthesis, characterization and application of silver nanoparticles using bioflocculant: A review. Bioeng. 11(5):492. doi:10.3390/bioengineering11050492.

Nkuwi EJ, Kabanangi F, Joachim A, Rugarabamu S, Majigo M. 2018. Methicillin-resistant *Staphylococcus aureus* contamination and distribution in patient's care environment at Muhimbili National Hospital, Dar es Salaam-Tanzania. BMC Res. Notes 11(1):1–6. doi:10.1186/s13104-018-3602-4.

Oprescu EE, Enascuta CE, Radu E, Ciltea-Udrescu M, Lavric V. 2022. Does the ultrasonic field improve the extraction productivity compared to classical methods – Maceration and reflux distillation? Chem. Eng. Process. - Process Intensif. 179:09082. doi:10.1016/j.cep.2022.109082.

Prasetyaningtyas T, Prasetya AT, Widiarti N. 2020. Sintesis nanopartikel perak termodifikasi kitosan dengan bioreduktor ekstrak daun kemangi (*Ocimum basilicum* L.) dan uji aktivitasnya sebagai antibakteri [Synthesis of chitosan modified silver nanoparticles with basil leaf extract (*Ocimum basilicum* L.) bioreductant and test of its activity as an antibacterial]. Indones. J. Chem. Sci. 9(1):37–43.

Rosman NSR, Masimen MAA, Harun NA, Idris I, Ismail WIW. 2021. Biogenic silver nanoparticles (AgNPs) from *Marphysa moribidii* extract: Optimization of synthesis parameters. Int. J. Technol. 12(3):635. doi:10.14716/ijtech.v12i3.4303.

Ruekit S, Srijan A, Serichantalergs O, Margulieux KR, Mc Gann P, Mills EG, Stribling WC, Pimsawat T, Kormanee R, Nakornchai S, Sakdinava C, Sukhchat P, Wojnarski M, Demons ST, Crawford JM, Lertsethtakarn P, Swierczewski BE. 2022. Molecular characterization of multidrug-resistant ESKAPEE pathogens from clinical samples in Chonburi, Thailand (2017–2018). BMC Infect. Dis. 22(1):695. doi:10.1186/s12879-022-07678-8.

Sahu N, Soni D, Chandrashekhar B, Satpute DB, Saravanadevi S, Sarangi BK, Pandey RA. 2016. Synthesis of silver nanoparticles using flavonoids: hesperidin, naringin and diosmin, and their antibacterial effects and cytotoxicity. Int. Nano Lett. 6(3):173–181. doi:10.1007/s40089-016-0184-9.

Sardjono RE, Gunawan R, Anwar B, Erdiwansyah, Mamat R. 2022. A mini review: Biosythesis of silver nanoparticles and its activity as antioxidant. Moroccan J. Chem. 10(4):808–821. doi:10.48317/IMIST.PRSM/morjchem-v10i3.30801.

Sarhan AS, Abdel-Hamid MI, Hanie R. 2022. Green synthesis of (CS/OLE) AgNPs and evaluation of their physico-chemical characteristic. Appl. Nanosci. 12(9):2765–2776. doi:10.1007/s13204-022-02538-y.

Septriani Y, Muldarisnur M. 2022. Kontrol ukuran nanopartikel perak dengan variasi konsentrasi ekstrak kulit buah manggis [Control of silver nanoparticle size with variation of mangosteen peel extract concentration]. J. Fis. Unand 11(1):68–74. doi:10.25077/jfu.11.1.68-74.2022.

Suhendra CP, Widarta IWR, Wiadnyani AAIS. 2019. Pengaruh konsentrasi etanol terhadap aktivitas antioksidan ekstrak rimpang ilalang (*Imperata cylindrica* (l) Beauv.) pada ekstraksi menggunakan gelombang ultrasonik [The effect of ethanol concentration on the antioxidant activity of ilalang rhizome extract (*Im-*

*perata cylindrica* (l) Beauv.) in ultrasonic wave extraction]. J. Ilmu dan Teknol. Pangan 8(1):27–35. doi:10.24843/itepa.2019.v08.i01.p04.

Sur UK, Ankamwar B, Karmakar S, Halder A, Das P. 2018. Green synthesis of silver nanoparticles using the plant extract of Shikakai and Reetha. In: Mater. Today Proc., volume 5. p. 2321–2329. doi:10.1016/j.matpr.2017.09.236.

Ulayya HF, Suwele YAL, Junior EI, Rinjani NA, Izat S, Suprapto S. 2019. Pemanfaatan lendir bekicot Afrika (*Achatina fulica*) sebagai obat luka bakar berbasis nanoemulsi [Utilization of African snail slime (*Achatina fulica*) as a nanoemulsion-based burn wound medicine]. Kartika J. Ilm. Farm. 6(2):91–94. doi:10.26874/kjif.v6i2.159.

Xia Q, Yang L, Hu K, Li K, Xiang J, Liu G, Wang Y. 2018. Chromium cross-linking based immobilization of silver nanoparticle coating on leather surface with broad-spectrum antimicrobial activity and durability. ACS Appl. Mater. Interfaces 11(2):2352–2363. doi:10.1021/acsami.8b17061.

Xu B, Azam SM, Feng M, Wu B, Yan W, Zhou C, Ma H. 2021. Application of multi-frequency power ultrasound in selected food processing using large-scale reactors: A review. Ultrason. Sonochem. 81:105855. doi:10.1016/j.ultsonch.2021.105855.

Yan X, He B, Liu L, Qu G, Shi J, Hu L, Jiang G. 2018. Antibacterial mechanism of silver nanoparticles in *Pseudomonas aeruginosa*: Proteomics approach. Metallomics 10(4):557–564. doi:10.1039/c7mt00328e.

Yanuar E, Umam K, Sarwana W, Huda I, Wijaya D, Roto R, Mudasir M. 2022. Preparation and *Vibrio* sp. antibacterial activity of silver nanoparticles mediated by *Chromolaena odorata* leaf extract using different temperatures. Asian J. Biol. 14(1):25–37. doi:10.9734/ajob/2022/v14i130203.

Yin IX, Zhang J, Zhao IS, Mei ML, Li Q, Chu CH. 2020. The antibacterial mechanism of silver nanoparticles and its application in dentistry. Int. J. Nanomedicine 15:2555–2562. doi:10.2147/IJN.S246764.